Evolutionary Intelligence
https://doi.org/10.1007/s12065-020-00491-9

RESEARCH PAPER

FAB classification of acute leukemia using an ensemble of neural networks

Jyoti Rawat[1] · Jitendra Virmani[2] · Annapurna Singh[3] · H. S. Bhadauria[3] · Indrajeet Kumar[4] · J. S. Devgan[5]

Received: 22 August 2019 / Revised: 22 May 2020 / Accepted: 3 September 2020

Abstract

Acute leukemia is the most frequently occurring malignancy present in human blood and a kind of liquid cancer. This hematological disorder can impinge on bone marrow and lymphatic system. Accordingly, a computer-aided classification system is proposed for French–American–British classification of Acute Leukemia using an ensemble of neural networks which is validated on 180 microscopic blood images taken from online benchmark dataset. As per the requirement of pathologists in real-life examination scenario various objectives are formulated as (i) correct nucleus segmentation in blood cell image, (ii) correct classification of FAB classes of acute leukemia (L1, L2, L3, M2, M3, and M5). To accomplish these research objectives the proposed method consist of segmentation section, feature extraction section, feature pruning section and classification section. The classification of the proposed method consists of two subsections as subsection1 is comprised of single six class PCA based neural network as PCA-NN0 (L1/L2/L3/M2/M3/M5) and subsection 2 contains an ensemble of 15 binary PCA based neural network classifiers as PCA-NN1 (L1/L2), PCA-NN2(L1/L3), PCA-NN3(L1/M2), PCA-NN4(L1/M3), PCA-NN5(L1/M5), PCA-NN6(L2/L3), PCA-NN7(L2/M2), PCA-NN8(L2/M3), PCA-NN9(L2/M5), PCA-NN10(L3/M2), PCA-NN11(L3/M3), PCA-NN12(L3/M5), PCA-NN13(M2/M3), PCA-NN14(M2/M5), PCA-NN15(M3/M5). The achieved accuracy for experiment 1 is 86.4% using PCA-NN0. The output of two most plausible classes predicted by PCA-NN0 is passed to other binary PCA based neural network i.e. PCA-NN1 to PCA-NN15. After passing all the test images to subsection 2, the achieved accuracy is 94.2% from the exhaustive experiment 2. The outcome of the work verifies the capabilities of computer-aided classification system to substitute the conventional diagnostic systems.

Keywords Acute leukemia · Leukemia classification · Feature extraction · Ensemble neural network

1 Introduction

The assessment of the peripheral blood smear is an imperative indicator of hematological and other unusual conditions that influence the body of a human being. In general, when most people hear the word cancer, then they usually think of a mass that is formed by rapid division of a group of cells. This mass can be seen by eyes and can be considered as the root of a problem that needs to be cured either through medicine or with surgery or chemotherapy. Due to this reason leukemia is difficult to visualize and understand as compared to other cancers [1, 2]. To be specific, leukemia is a blood cell cancer that contains red blood cells (RBCs) that are required for carrying the oxygen, platelets which are not cells but the chunk of cells that stops bleeding through the formation of blood clots and various kinds of white cells that are required to provide immunity. These cells constitute blood cells but are not made inside the blood but instead inside the bones. If the bone is analyzed, it is observed that the bones are not solid throughout and consists of a hollow cavity at their center which is filled with spongy red tissue that is called bone marrow. It is where these types of blood cells are produced. Figure 1 is illustrating the difference between normal blood cell and cancerous blood cell.

✉ Jyoti Rawat
drjyotirawat19@gmail.com

1 DIT University, Dehradun, Uttarakhand, India

2 CSIR-Central Scientific Instruments Organization, Chandigarh, India

3 G.B. Pant Institute of Engineering and Technology, Pauri Garhwal, UK, India

4 Graphic Era Hill University, Dehradun, Uttarakhand, India

5 M. M. Institute of Medical Sciences and Research, Solan, HP, India

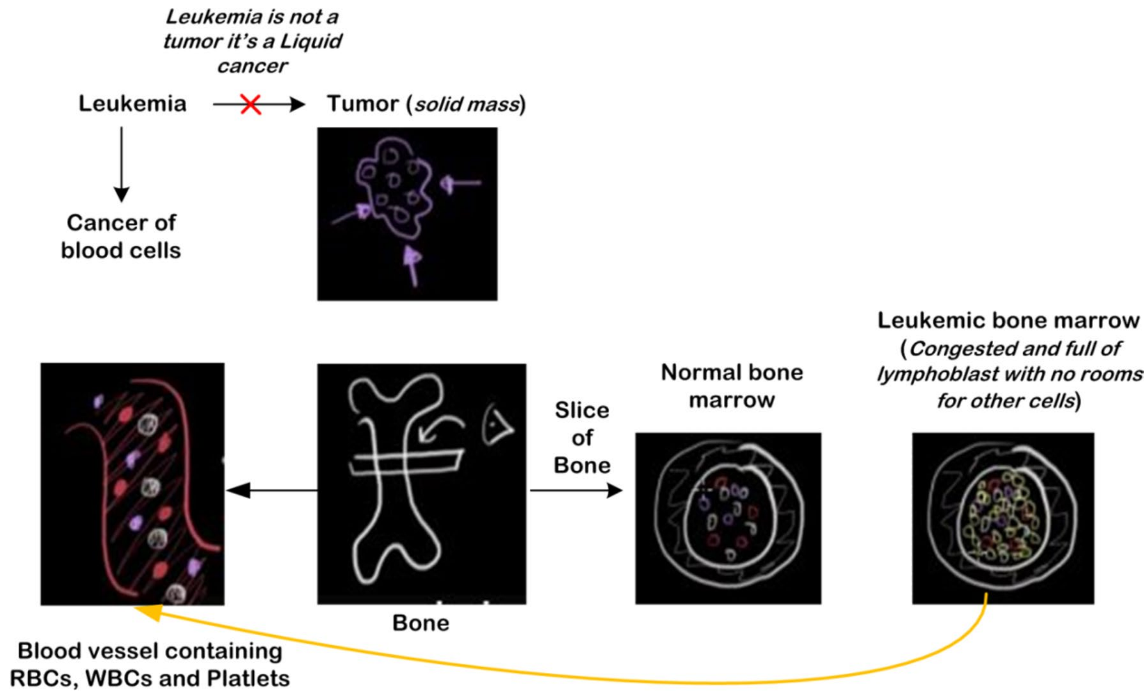

Fig. 1 Formation of Leukemic cells in bone marrow [2]

Inside the bone marrow, it can be seen that in normal cases platelets, red and white blood cells are being made while in case of leukemia, any of the platelets, red or white blood cells start multiplying way faster than the normal and overtake the bone-marrow as seen in Fig. 1. That results in mainly two abnormalities, firstly, the rapidly dividing cells that constitute leukemic cell causes malfunctioning of normal cell i.e. if these are red blood cells then they would not carry oxygen, if are white cells then they would not provide any immunity and if platelets then they would not form any kind of blood clots. Thus, it leads to wastage of energy and space inside the bone-marrow as it is being used to produce the cells that occupy the entire circulatory system but does not perform its function. Secondly, if any of these cells divide rapidly then a lot of space is occupied inside the bone-marrow leaving very narrow space to food for remaining cells which is required for their growth and this disables bone-marrow from producing the required amount of healthy cells and lacks in supplying healthy cells into the blood which ultimately causes problems of fewer WBCs, RBCs and platelets within the blood and leads to improper functioning of these cells irrespective of the blood cell subjected to cancer.

Later, when leukemic cells are short of space for growth within the bone-marrow then they would leak out into blood [1, 2], and thus different types of cells are present in the blood which areproducedwithin the bone marrow. Moreover, all of these different cells originate from the same cell called a hematopoietic stem cell. This hematopoietic stem cell can segment into any type of blood cell, and this newly made immature cell is known as blast cell which is big and has a large nuclei.

As it can be seen, the nucleus occupiesalmost the entire cell and comprise of disorganized and loose DNA but the cell doesn't stay immature forever. Eventually, it shrinks in size along with DNA in such a manner that the nucleus takes up a smaller portion of the cell and even the DNA inside the nucleus changes in appearance and becomes more organized. The cell matures through various stages until it reaches its final stage where it is a lot smaller than earlier and the DNA inside the nucleus is present in compacted and organized manner. Acute leukemia generally affects the most immature growth stage of blood cells. ALL (Acute lymphoblastic leukemia) is the most common type of cancer among children and is generally associated with people with Down syndrome.

Basic symptoms of leukemia are (i) fewer erythrocytes (fatigue, shortness of breath, pale skin), (ii) fewer thrombocytes (easy bruising) and (iii) fewer leukocytes (infections) and due to rapid division of these leukemic cells which consumes a lot of energy, the symptoms like (iv) significant weight loss (v) weakness. Moreover, leukemia cells ultimately start to propagate into the wall of the bone that results in bone pain thought out the body.

The morphology of acute leukemias (AML and ALL) in clinical manner with elaboration of different characteristics of various classes (L1, L2, L3, M2, M3 and M5) of acute leukemia is explained in Fig. 2.

Once a patient begins to show the symptoms associated with leukemia, the doctor will generally get the blood test of that patient done where the lack of healthy cells or in some

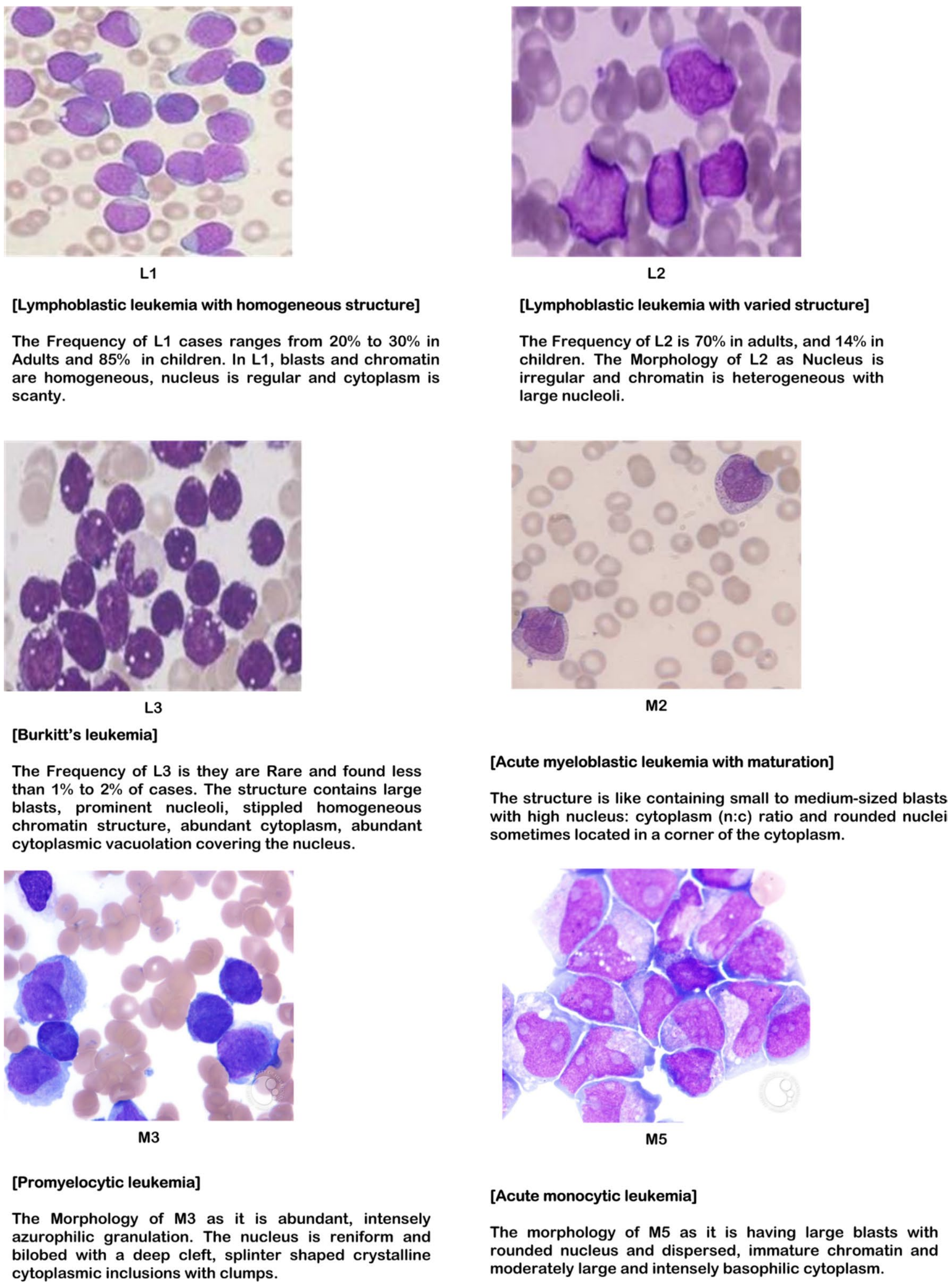

Fig. 2 French–American–British (FAB) classification of acute myeloblastic leukemia and acute myeloblastic leukemia

cases the leukemic cells can be observed in blood as well. This observation leads to the anonymity of patient being leukemic and needs to be confirmed through observing the insides of bone-marrow which is done by microscopic analysis of bone marrow by hematologist which is a tedious task. To automate the process and to assist the expert, there is a requirement of computer-aided classification tool that would be able to categorize the FAB subtypes of acute leukemia [2].

The FAB is the international standard that classifies the leukemia disorder into Acute Lymphoblastic Leukemia or ALL and Acute Myeloblastic Leukemia or AML. Then these two classes further classified into their subtype as ALL divided into 3 subclasses L1, L2, L3, and AML can be categorized into 8 subtypes, M0–M7 based on the maturity of blood cell into bone marrow [15]. This work focuses on classifying the FAB subclasses of acute leukemia into six classes as L1, L2, L3, M2, M3 and M5.

2 Literature review

The literature perceives that a variety of classification frameworks exist for the identification of leukemic cell from the normal one [3–30]. The literature regarding the classification of leukemia and their subclasses tabulated in Figs. 3, 4, 5, 6 based on different extracted features as single features as *texture only*, *shape only* as well as combined feature extraction methods as *texture* + *shape*, *texture* + *color*, *shape* + *color*, *texture* + *shape* + *color*according to available state of art methods.

Figure 3 illustrated the literature related to the existing classification frameworks that are able to classify the normal blood cells from the ALL (Acute lymphoblastic Leukemia) cells. The study observed that the highest classification accuracy for the normal blood cells and ALL cells is 99.2% obtained in the study [3] using SVM (support vector machine).

In Fig. 4, studies associated with classification of normal blood cells and AML cells. From Fig. 4, the maximum precision for the classification of normal blood cells and AML cells is 98% observed [22, 23], that is obtained through extraction of different shape, texture features and colour from both types of cells images using the classifier like SVM. In Fig. 4, the existing studies are alienated into three parts as (i) *shape* + *texture* feature-based studies that represented by only one study with the accuracy of 97% [24], (ii) *shape* + *texture* + *color* feature-based studies that include two studies with a maximum accuracy of 98% [23, 25] and (iii) *texture-based* study that includes one study with the highest accuracy of 98% [22].

There is only one study [27] in which ALL and AML classes are discriminated by extracting the texture and shape features only. It also depicted four studies [26, 28–30], in which computer-aided classification system classified the ALL and AML classes by obtaining the multiple features on segmented cell images as shape, color and various texture features.

Similarly, In Fig. 5, the uppermost accuracy of 99.8% is obtained for AML and ALL classification by applying SRG classifier [26].

In Fig. 6, the studies are done on acute leukemia classification. The first study is based on the hierarchical classification problem. In which all images are discriminated in the acute myeloid leukemia (AML), acute lymphoid leukemia (ALL) from the normal cell images. Additionally, these classes are classified into their FAB classification as AML into M2, M3, and M5 and ALL into L1, L2, and L3 applying various SVM kernels. This study reveals the overall accuracy of 98.3%. Sometimes it is not suitable to perform hierarchical classification by the pathologist for some classification problems where classes are atypical in most cases; they need a classification framework for multiclass characterization. At this point of time accuracy is not a matter of concern, there would be a need of CAC system based on the multiclass classifier. Therefore, the present study represents a multiclass classification framework. The second study is a multiclass classification based on an ensemble of neural network classifier and discriminates six classes of acute leukemia into L1, L2, L3, M2, M3 and M5 respectively.

From the broad study of background and literature, it can be observed that there is less work available regarding the present problem where all the normal cell is distinguished from leukemic cells and later the leukemic cell is classified into AML and ALL cells with additional sub-classification of AML and ALL cells into their FAB classes (M2, M3, M5, L1, L2 and L3).

The main objectives of current work are (i) segmentation of nucleus (ii) extraction of shape, texture and colour features of the nucleus (iii) six-class(L1, L2, L3, M2, M3, and M5) classification of acute leukemic cells. To accomplish these purposes, the nucleus of white blood cell is extracted from the background of the cell. Then many types of features are calculated from the segmented image of the nucleus for precise classification. Then an ensemble binary ANN classifier is used to recognize six classes of acute leukemia.

The outcome of this study illustrates that the present method used with the amalgamation of various feature vectors assists to discriminate between dissimilar acute leukemia types with an overall accuracy above 90%.

Normal/ALL classification system

Shape+Texture feature based CAC system

Author s/Year	Singh, G. et al. 2016, [6]	Amin, M.M., et al. 2015, [8]	Mohapatra, S. et al. 2010, [12]	Mohapatra, S. et al. 2011, [16]	Madhloom, H.T et al. 2012, [17]	Lorenzo Putzu et al. 2014, [18]	Putzu, L. et al. 2013, [19]	Rawat, J. et al. 2015, [20]
No. of Images	108	21	108	108	260	267	245	196
Classifier	ANN	SVM	SVM	SVM	ANN	SVM	SVM	SVM
Dataset	ALL-IDB	Omid hospital	Ispat General Hospital, Rourkela, India	Ispat General Hospital, Rourkela, India	University of Malaya, Malaysia	ALL-IDB	ALL-IDB	ALL-IDB
Accuracy	97.2	97.0	95.0	93.0	92.5	92.0	92.0	89.8

Texture+Shape+Color feature based CAC system

Authors/ Year	Rawat J. et al. 2017, [3]	Viswanathan, P. et al. 2015, [5]	Neoh, S.C., et al. 2015, [9]	Mohapatra, S. et al. 2014, [14]
No. of Images	260	108	180	104
Classifier	SVM	Fuzzy C means classifier	Dempster-Shafer	EOC*
Dataset	ALL-IDB	ALL-IDB	ALL-IDB	Ispat General Hospital, Rourkela, India
Accuracy	99.2	98.0	96.7	94.7

Texture feature based CAC system

Authors/Year	Singhal, V. et al. 2016, [15]
No. of Images	260
Classifier	SVM
Dataset	ALL-IDB
Accuracy	93.8

Shape feature based CAC system

Authors/Year	Bhattacharjee, R. et al. 2015, [11]	Zhang, L. et al. 2016, [7]	Scotti, F. et al. 2005, [21]
No. of Images	120	--	113
Classifier	ANN	Fuzzy system	FFNN
Dataset	ALL-IDB	Harbin Medical University, China	M. T Research Centre, Italy
Accuracy	95.2	--	75.9

Shape+ Color feature based CAC system

Authors/Year	Aimi, A.N. et al. 2013, [10]
No. of Images	230
Classifier	MLP_BR
Dataset	--
Accuracy	95.7

Other feature based CAC system (Fractal dimensions, colour and shape features*) (Multiple clinical, laboratorial features#)

Authors/Year	Mohapatra, S. et al. 2010, [13]*	Pedreira, C.E et al. 2012, [4]#
No. of Images	108	189
Classifier	SVM	ANN
Dataset	Ispat General Hospital, Rourkela, India	Federal University of Rio de Janeiro (UFRJ)
Accuracy	95.0	98.2

Fig. 3 State of art available for the Normal blood cells and Acute lymphoblastic leukemia classification

3 Material and methods

3.1 Database description

To build up an automated classification system for leukemia, one need to train the classifiers with wide-ranging data sets tends to represent each subclass of leukemia. In this study, a combined set of images has taken from the online image repositories as American society of hematology (ASH) and ALL-IDB [31, 32]. The database for this study contains total 280 sub-images or region of interest (ROIs) including different kind of leukemia subclasses as

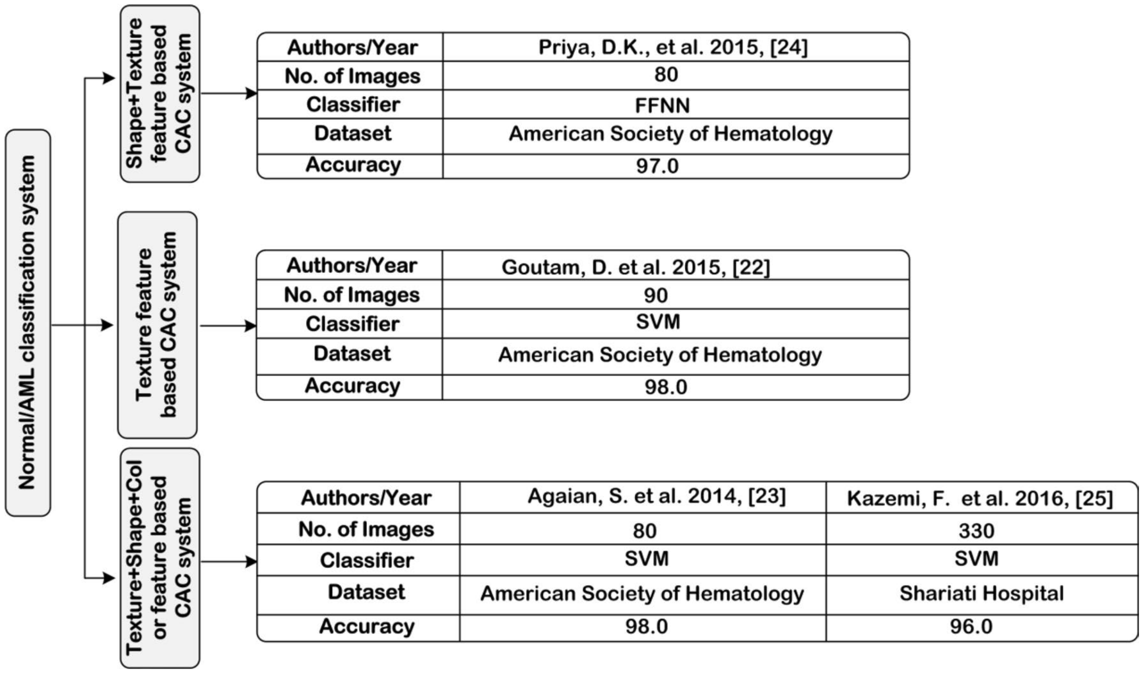

Fig. 4 State of art available for the Normal blood cells and Acute Myeloblastic leukemia classification. EOC-Ensemble of Naive Baiyes, *k*NN, MLP-SVM, RBFN-SVM and SVM classifiers. L1, L2, and L3 are the FAB classes of Acute lymphoblastic leukemia (cancerous cell)

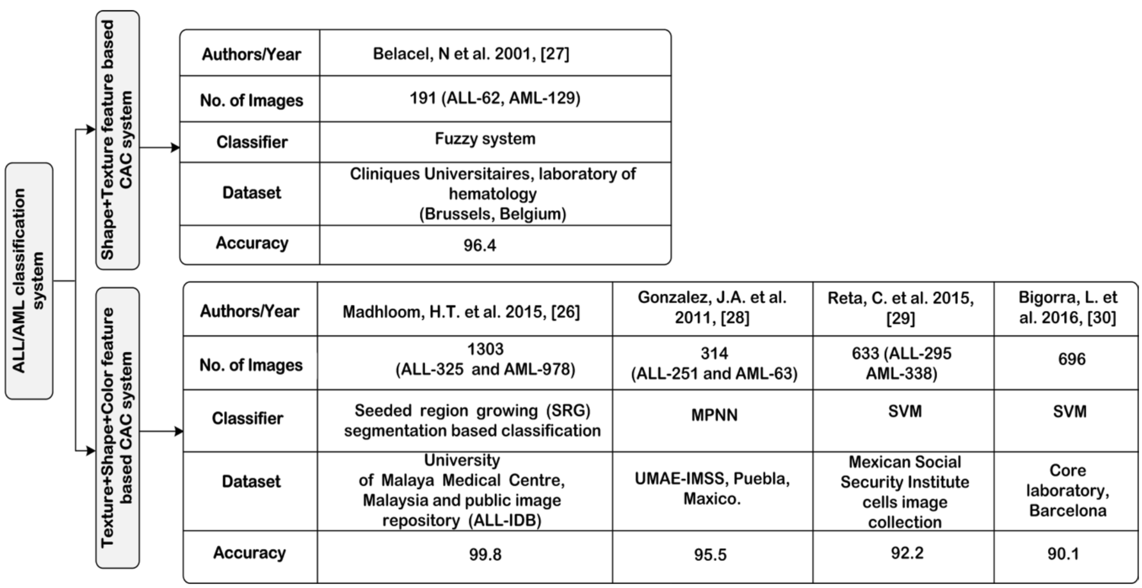

Fig. 5 State of art available for the AML and ALL classification. EOC Ensemble of Naive Baiyes, *k*NN, MLP-SVM, RBFN-SVM and SVM classifiers.L1, L2 and L3 are the FAB classes of Acute lymphoblastic leukemia (cancerous cell)

64 sub-images of L1, 46 sub-images of L2, 30 sub-images of L3, 54 sub-images of M2, 38 sub-images of M3 and 48 sub-images of M5. Additionally, these images are labeled by the participating hematologists and classification of ground truth into six class's i.e. L1, L2, L3, M2, M3 and M5.

The short depiction of used dataset and its divergence in testing and training set is illustrated in Fig. 7.

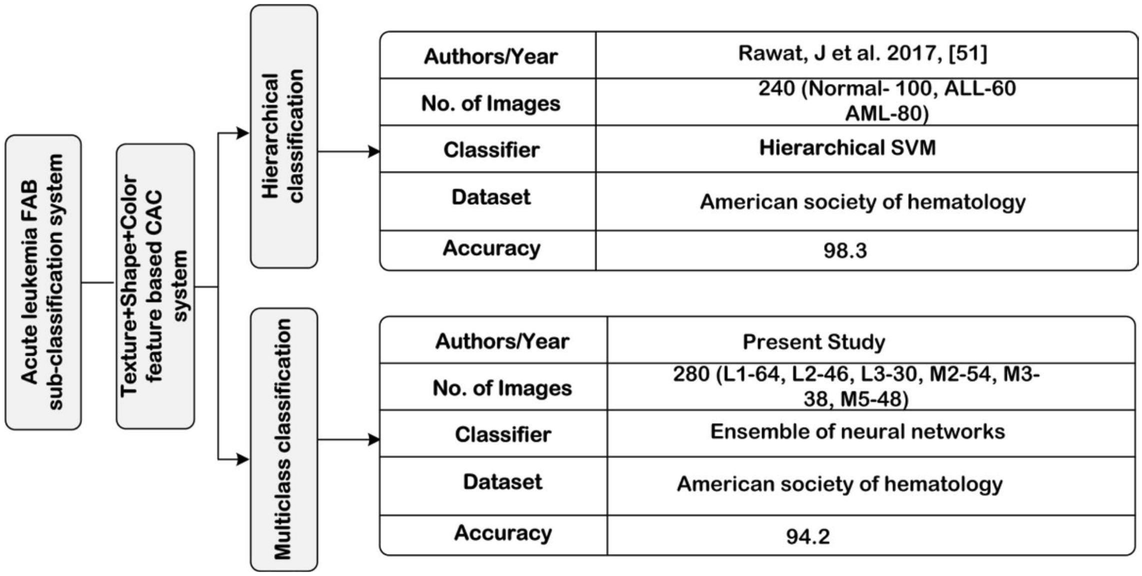

Fig. 6 State of art available for the Acute leukemia classification

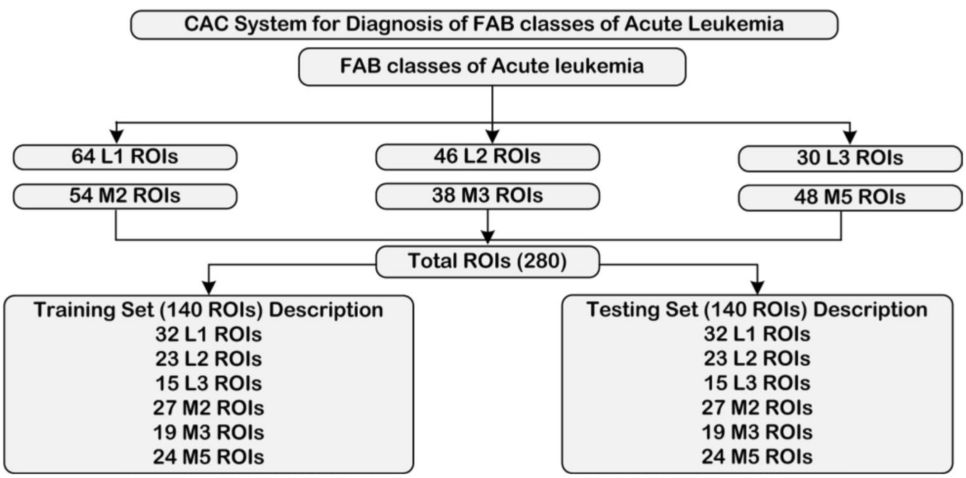

Fig. 7 Dataset and their division into testing and training sets

3.2 Proposed acute leukemia classification framework

The acute leukemia classification is represented through the diagram given in Fig. 8. The proposed method contains various modules i.e. segmentation, feature extraction, feature selection and their classification. Here, first of all, segmentation is done for the separation of nuclei from the cell background. Then various features are extracted to detect the morphological, chromatic and textural distinctions between different classes of the acute leukemic cell, it is followed by the process of feature selection. After selecting some prominent features, all the selected features fed into the classifier to obtain the correct classification result. The brief details of each module are specified in subsequent segments.

3.2.1 Segmentation module

After preprocessing and de-noising, segmentation is the next step which allows separating the region of interest (nucleus part) from the cell image and gets ready to apply techniques for different operations like features extraction, selection and their classification [3, 33]. In the present work, the PCA fusion-based hybrid method of segmentation is implemented. Consequently, this step slices the object of interest i.e. nucleus from the cell image. The input cell image is cropped using the nominal rectangle to completely hold a connected part based on intensity values is utilized to distinguish a required cell nucleus in every sub-image as is represented in Fig. 9.

The algorithm with steps regarding the segmentation of sub-image is depicted in Fig. 10.

Fig. 8 Proposed Acute leukemia classification framework

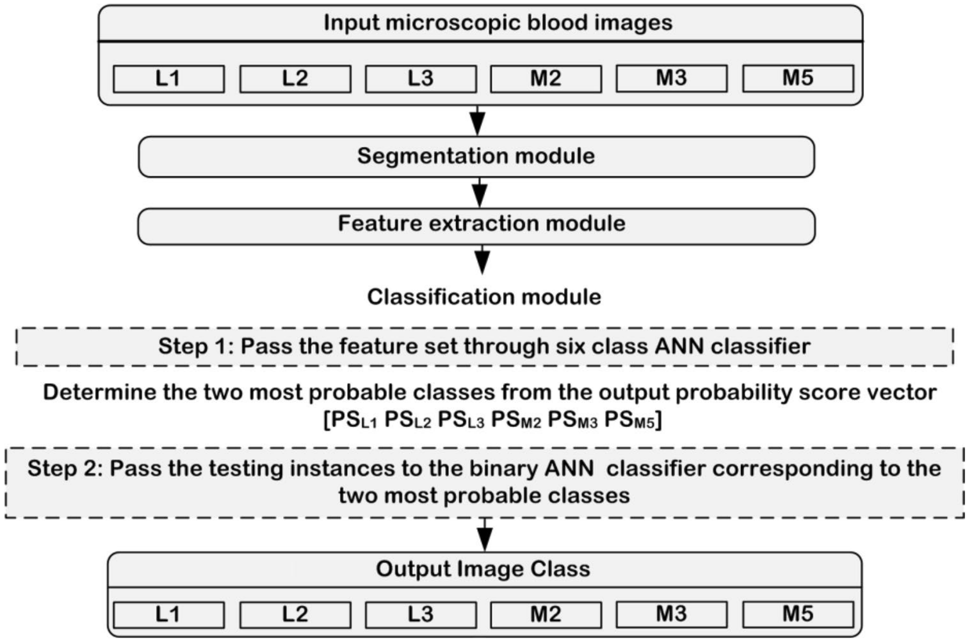

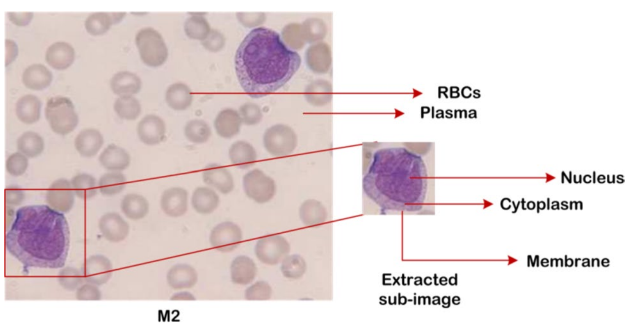

Fig. 9 Nuclei sub-image selection of input cell image

The quality of medical images can interfere with different noises. Therefore, image pre-processing is required that includes noise removal and enhancement. In this segmentation method, input sub-image is converted into gray scale, and then other enhancements and morphological operations are performed. The brief depiction is represented in Fig. 11 and discussed in the study [3].

3.2.2 Feature extraction module

Extracting the different feature descriptors of any image is a well-known method and optimized in various pattern recognition and image processing areas. However, the selection of prominent features for the recognition of leukemic cells from

Fig. 10 Algorithm for Segmentation of nucleus using hybrid segmentation method

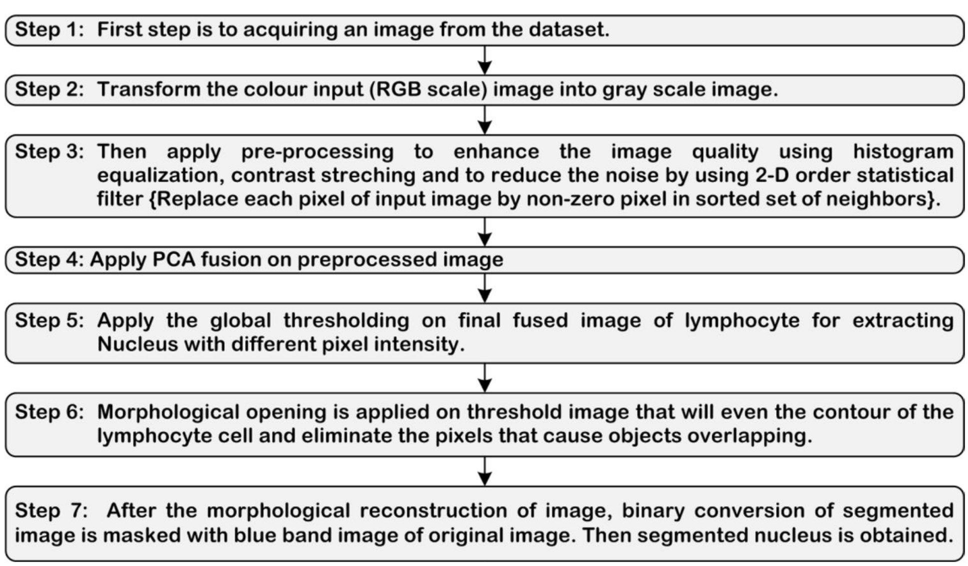

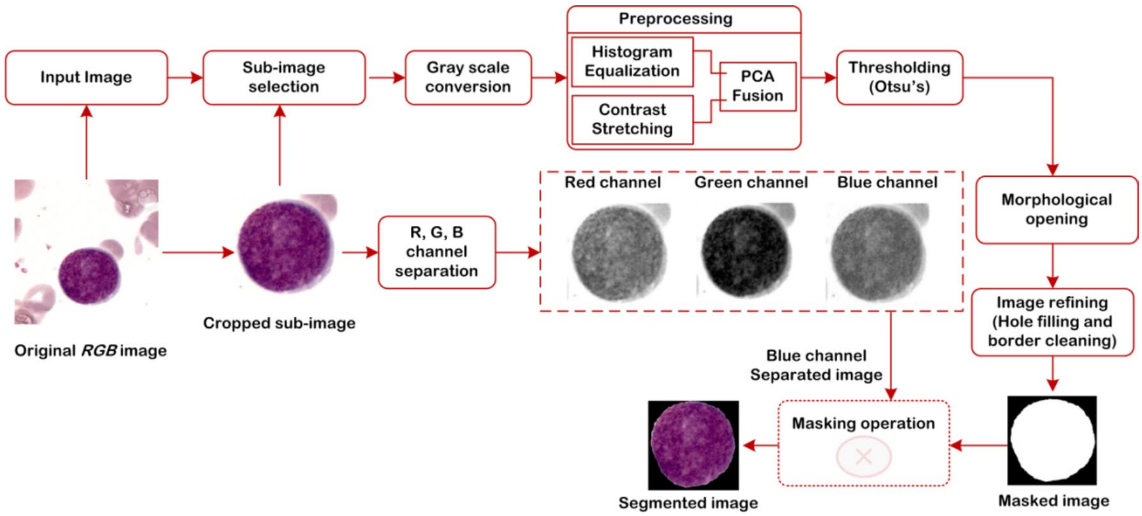

Fig. 11 Segmentation of nucleus region

the pathological images is the major difficulty. The foremost step for the extraction of features is to select the strongest associated and correlated to the predicted classes and to choose the strong feature descriptor with the ability of high discrimination [34–42]. In this work, various texture, shape features and colour are grouped for separating six classes of acute leukemia.

The objective of this research is to provide an advance blood cell characterization method even in the existence of deprived quality or low magnification blood cell images. In order to differentiate among leukemic cells types, computation of different features of the input sub-images that lead to enhanced separability of six-classes by classifiers is needed. Combining various individual features collectively permits to recompense rate of error and increases their classification consistency to certain level.

The brief explanation of the extracted features is tabulated in Fig. 12

3.2.3 Feature reduction through Principal component analysis (PCA)

The unnecessary dimensionality of various features can increase the cost of computation; the combination of nonlinear or linear features has been applied through high dimensional data projection on space with lower dimensions that has also optimized the classifier correctness [43, 79]. Different methods for reduction of non-linear dimensionality are introduced for maintaining the finest features and components. In present work, PCA is implemented on complex and immense dimensional spaced feature vectors in order to deduce it into simplified and compact space dimensionality for efficient analysis of features by using the principal component structure of the given set. The deviation is observed in results of classification when varying values for PC are used on the set of extracted features by implementing PCA [3, 79]. This deviation of projection for each PC value can be measured through its Eigenvalue. In the given problem, each existing subset of the feature vector of different size of feature descriptor for shape, texture and colour are taken into consideration for feature selection. In order to evaluate optimum value for PC, the broad number of experiments are done for every classification by taking value for pc ranging from 2 to 15 i.e. initially pc is taken as 2,3,4,…, 15. The brief working steps for PCA is given in Fig. 13.

3.2.4 Classification module

The classification section of the proposed method consists of 2 subsections as (i) subsection1 is comprised of single six classed PCA neural network as PCA-NN0 (L1/L2/L3/M2/M3/M5) and Sect. 2 contains an ensemble of 15 binary PCA based neural network classifiers as PCA-NN1 (L1/L2), PCA-NN2 (L1/L3), PCA-NN3 (L1/M2), PCA-NN4 (L1/M3), PCA-NN5 (L1/M5), PCA-NN6 (L2/L3), PCA-NN7 (L2/M2), PCA-NN8 (L2/M3), PCA-NN9 (L2/M5), PCA-NN10 (L3/M2), PCA-NN11 (L3/M3), PCA-NN12 (L3/M5), PCA-NN13 (M2/M3), PCA-NN14 (M2/M5), PCA-NN15 (M3/M5) used in classifying blood cell images as L1, L2, L3, M2, M3 and M5. The implemented module is given in Fig. 14. The detailed study of an artificial neural network is available in different research works [44–52].

Classification module one It comprises of a six-classed PCA ANN classifier (PCA-NN0) gives probability score vector (PSV) for the testing object to the corresponding class. Feature reduction module takes input feature space for simplification of its dimensionality. The ideal pc value is evaluated by taking a range of values from 2 to 15.

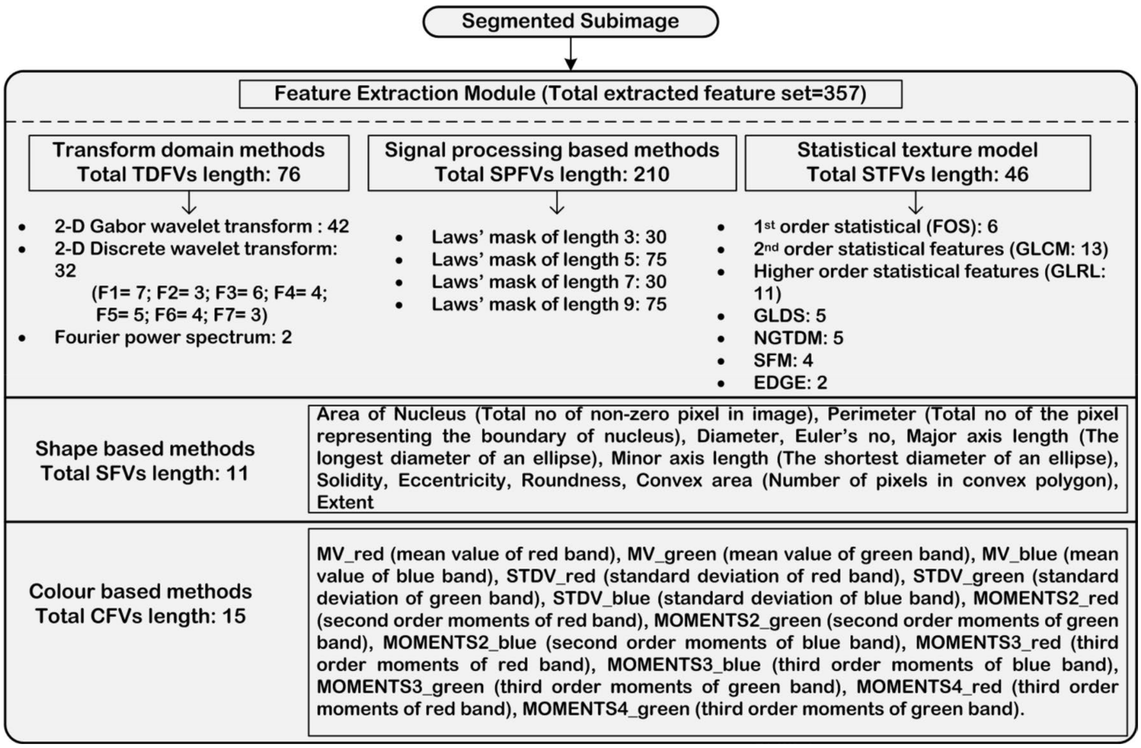

Fig. 12 The list of total extracted features for classification of Acute leukemia. *TDFVs* Transform domain feature vectors; *SPFVs* Signal processing based feature vectors; *STFVs* Statistical texture feature vectors; *SFVs* Shape feature vectors; *CFVs* Colour feature vectors

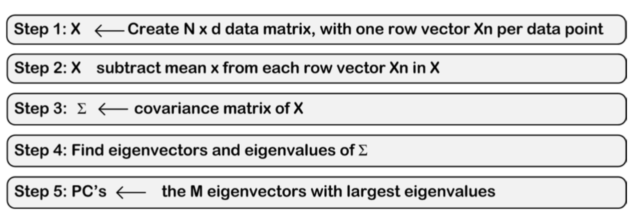

Fig. 13 Working steps for PCA

PCA-NN0 performance is depicted in Table 1. The division of instances of each class of testing and training data for the given classifier is represented in Fig. 15.

Classification module two It comprises of an ensemble of fifteen mutually independent binary ANN classifiers i.e. [PCA-NN1 (L1/L2), PCA-NN2 (L1/L3), PCA-NN3 (L1/M2), PCA-NN4 (L1/M3), PCA-NN5 (L1/M5), PCA-NN6 (L2/L3), PCA-NN7 (L2/M2), PCA-NN8 (L2/M3),

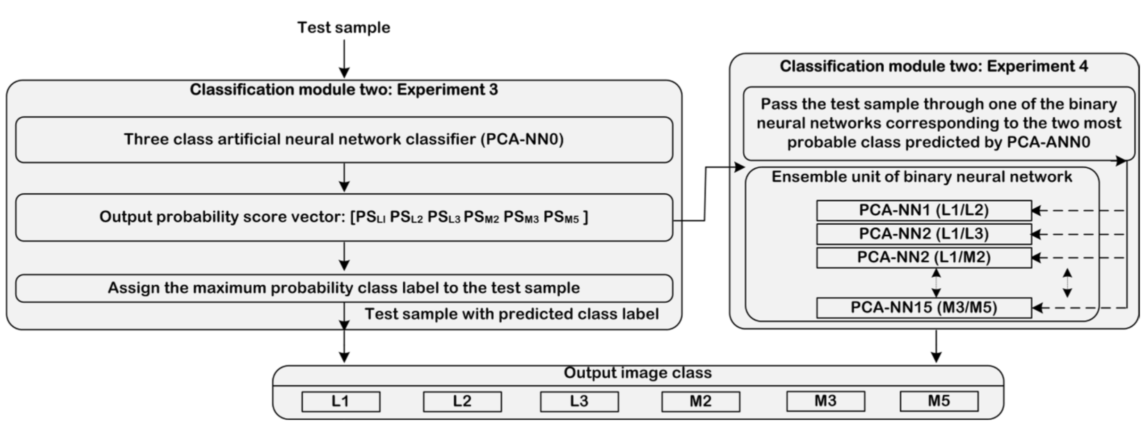

Fig. 14 Architecture of module for Acute leukemia classification

Table 1 Description of each neural network model, training accuracy and optimal number of pc value

Experiment no.	Model no.	'*pc*' value	Description of neural network layers (I:H:O)	Training accuracy (%)
Experiment 1	PCA-NN0	8	331:10:6	86.4
Experiment 2	PCA-NN1	6	331:10:2	100
	PCA-NN2	10	331:10:2	98
	PCA-NN3	11	331:10:2	97.3
	PCA-NN4	8	331:10:2	100
	PCA-NN5	7	331:10:2	98.6
	PCA-NN6	5	331:10:2	99.6
	PCA-NN7	4	331:10:2	95.5
	PCA-NN8	3	331:10:2	100
	PCA-NN9	6	331:10:2	100
	PCA-NN10	8	331:10:2	100
	PCA-NN11	9	331:10:2	100
	PCA-NN12	12	331:10:2	99.6
	PCA-NN13	7	331:10:2	99.3
	PCA-NN14	9	331:10:2	99.6
	PCA-NN15	13	331:10:2	100

pc principal component value, I:H:O: Input: Hidden: Output layer

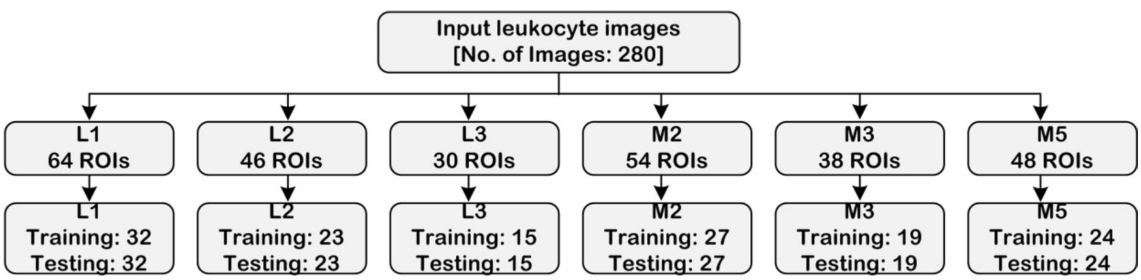

Fig. 15 Division of instances of each class of training and testing data for classifier PCA-NN0

PCA-NN9 (L2/M5), PCA-NN10 (L3/M2), PCA-NN11 (L3/M3), PCA-NN12 (L3/M5), PCA-NN13 (M2/M3), PCA-NN14 (M2/M5), PCA-NN15 (M3/M5)] used in classifying input images as L1, L2, L3, M2, M3 and M5. Two labels of classes with the highest probability are decided through PSV given by PCA-NN0, which are then used as input to corresponding binary PCA-NN to perform classification in these two classes. The ideal pc value is evaluated by taking a range of values from 2 to 15 for every NN based classifier.

Artificial neural network classifier

The artificial neural network is inspired by biological neural network which processes given input to produce the corresponding output based on the intelligence of the organism. This biological neural network has a basic processing unit called a neuron. This neuron serves as a basis for the development of artificial neuron and a group of these neurons can be utilized to work together through a network for processing given set of inputs. This network is what constitutes artificial neural network, and can be made more accurate by implementing three ideas [53–58].

The basic architecture of ANN classifier is illustrated in Fig. 16, gives details of working of the neural network, its topology, different layers and various variables representing the weights that each connection associates with each input of the respective layer.

A time-scale element is subjected to the majority of the neural system inactivity rule, local standards characterize the way neuron activities changes due to one-another. In this system, the action principle of each layer depends regularly on the weights [54–60]. The change in these weights associated with two corresponding layers determines the learning principle which occurs generally on an extended time scale as compared to the time size related to the movement standards.

Image processing has improved with broader use due to neural system restoration that is introduced through

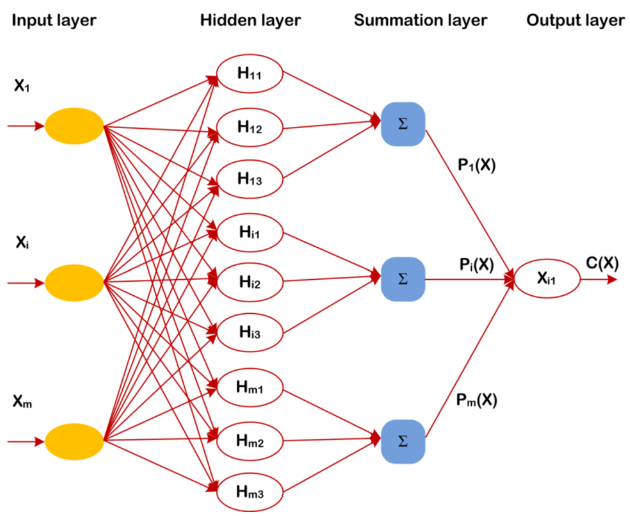

Fig. 16 Architecture of ANN classifier

various statistical pattern recognition methods introduction. Initially, linear and quadratic discriminant and Parzen density estimator were used for unraveling the pattern recognition issues [61–78]. Moreover, feature extraction is must if the object for recognition is worthwhile and must be analyzed deeply. If anything, else is used then the classification cannot produce as a reliable result as are yielded from the feature extraction modules.

The division of instances of each class of training and testing data for given classifiers is represented in Fig. 17.

The ideal pc value which produces highest accuracy for the classification in every binary ANN is shown in Table 1.

3.2.5 Experiments and results

3.2.5.1 Environmental setup The complete dataset are kept at HP Z420 workstation and MATLAB-2018 environment is used for performing the experiments. The specification of the used workstation is mentioned as Intel Xeon e5-1607, CPU @ 3.0 GHz, 16 GB RAM, NVIDIA QUADRO and 512 GB SSD.

3.2.5.2 Result analysis ***Experiment 1*** It comprises of a six-class PCA ANN classifier (PCA-NN0) that gives the PSV (probability score vector) of test sample which belongs to a specific class. The highest value of PSV is allocated to a test sample class label. The performance of six-class PCA-NN0 is mentioned in Table 2.

From Table 2, it is observed that overall classification accuracy (OCA) for the given classifier is 86.4% (121/140). It depicts that 121 of 140 test instances are accurately classified. The individual class accuracy (ICA) is 93.7% (30/32), 86.9% (20/23), 86.6% (13/15), 85.1% (23/27), 84.2% (16/19), and 79.1% (19/24) for L1, L2, L3, M2, M3 and M5, respectively.

From the experiment 1, it has been observed that the 19 of 140 testing instances are inaccurately classified. Among 19 misclassified instances, 2 instances belong to L1 is classified as L2 & L3, 3 instances belong to L2 is classified as L1 & L3, 2 instances belong to L3 is classified as L2, 4 instances belong to M2 is classified as M3 & M5, 3 instances belong to M3 is classified as M2 & M5 and 5 instances belong to M5 class is classified as M2% M3. These misclassified instances are passed to the next level according to their PSV values. Table 3 describes each of these 140 instances following output of module one.

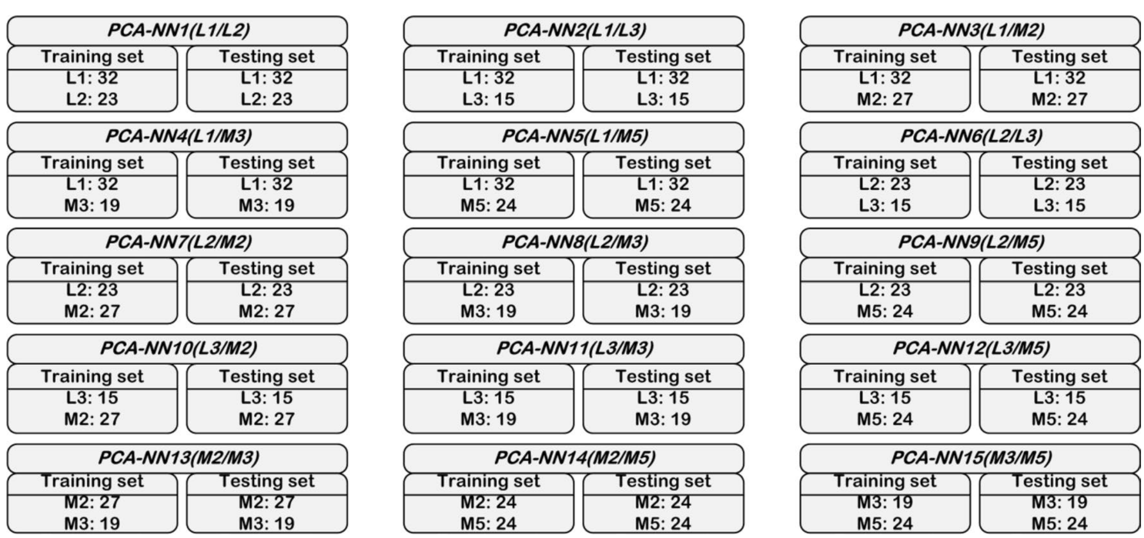

Fig. 17 The division of instances for each class of testing and training data for ensemble of fifteen binary classifiers (PCA-NN1 to PCA-NN15)

Table 2 Results of module one (PCA-NN0) classifier

	CM						Accuracy (%)						
	L1	L2	L3	M2	M3	M5	OCA	ICA_{L1}	ICA_{L2}	ICA_{L3}	ICA_{M2}	ICA_{M3}	ICA_{M5}
L1	30	1	1	0	0	0	86.4	93.7	86.9	86.6	85.1	84.2	79.1
L2	1	20	2	0	0	0							
L3	0	2	13	0	0	0							
M2	0	0	0	23	3	1							
M3	0	0	0	2	16	1							
M5	0	0	0	2	3	19							

CM confusion matrix; *OCA* overall classification accuracy; ICA_{L1} individual class accuracy for L1; ICA_{L2} individual class accuracy for L2; ICA_{L3} individual class accuracy for L3; ICA_{M2} individual class accuracy for M2; ICA_{M3} individual class accuracy for M3; ICA_{M5} individual class accuracy for M5

Table 3 Description of 140 test instances in accordance with results produced by module one

Total testing instances	Accurately classified instances[#]	Misclassified instances	Instances with 2nd highest probability for accurate class	Instances with 3rd highest probability for accurate class	Instances with 4th highest probability for accurate class	Instances with 5th highest probability for accurate class	Instances with 6th highest probability for accurate class
L1: 32	30	2	2	0	0	0	0
L2: 23	20	3	2	1	0	0	0
L3: 15	13	2	1	1	0	0	0
M2: 27	23	4	2	1	1	0	0
M3:19	16	3	1	1	1	0	0
M5:24	19	5	3	2	0	0	0
Total: 140	121	19	11	6	2	0	0

Accurately classified instances[#]: instances with most probability

The output PSV of the classification module one, PCA-NN0 gives probability score related to every test sample for corresponding class. From Table 3, it is observed that 19 wrong classified instances consists of 2 instances of L1, 3 instances of L2, 2 instances of L3, 4 instances of M2, 3 instances of M3 and 5 instances of M5.

Experiment 2 In this experiment, the output PSV [$PS_{L1,}$ $PS_{L2,}$ $PS_{L3,}$ $PS_{M2,}$ PS_{M3} and PS_{M5}] yielded through PCA-NN0 the number of testing instances that pass through the each binary PCA-NN classifier is shown in Fig. 18.

After the passing each test sample through the respective binary PCA-NN classifier, the obtained results given in Table 4. It depicts the accurate or inaccurate classification of testing instances by module 2.

The results obtained from experiment 2 shows 132 out of 140 test instances are classified accurately while remaining 8 i.e. (140–132) were inaccurately classified by implementing module 2. Inaccurately classified instances can be calculated by:

$$TMIs = \sum_{i=1}^{15} MIs(PCA - NN_i)$$

or

$$TMIs = \sum MIs(PCA - NN1), MIs(PCA - NN2), \dots , MIs(PCA - NN15) \quad (1)$$

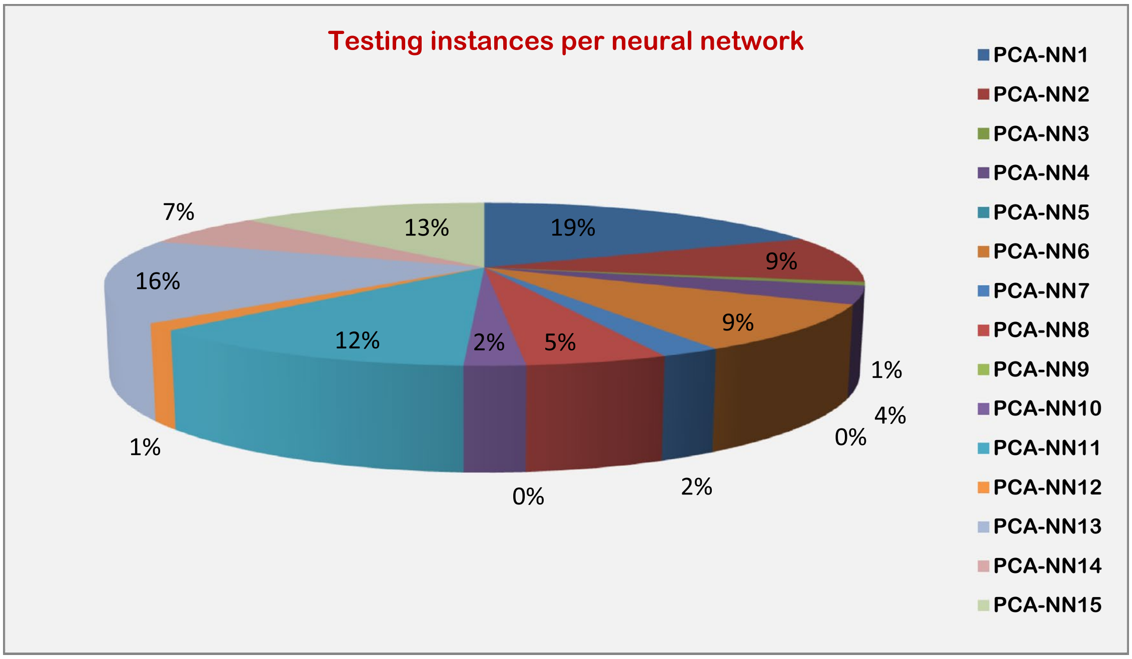

Fig. 18 The total number of testing instances that passes through the each binary PCA-NN classifier

Table 4 Description of accurate or inaccurate classification of testing instances by module 2

Binary neural network	Testing instance		Instances description	
	No. of instances	Description	No. of Classified	No. of Misclassified
PCA-NN1	26	26 of L1	26 of L1	–
PCA-NN2	13	13 of L3	12 of L3	1 of L3 is misclassified as a L1
PCA-NN3	1	1 of L1	1 of L1	–
PCA-NN4	5	5 of L1	5 of L1	
PCA-NN5	–	–	–	–
PCA-NN6	13	13 of L2	13 of L2	1 of L2 is misclassified as a L3
PCA-NN7	3	3 of L2	2 of L2	–
PCA-NN8	7	7 of L2	7 of L2	–
PCA-NN9	–	–	–	–
PCA-NN10	3	3 of M2	2 of M2	1 of M2 is misclassified as a L3
PCA-NN11	17	17 of M3	15 of M3	1 of M3 is misclassified as a L3 and 1 of M3 is misclassified as a M5
PCA-NN12	2	2 of L3	2 of L3	–
PCA-NN13	23	21 of M2, 2 of M3	20 of M2 and 2 of M3	1 of M2 is misclassified as an M3
PCA-NN14	9	3 of M2, 6 of M5	3 of M2 and 5 of M5	1of M5 is misclassified as a M2
PCA-NN15	18	18 of M5	17 of M5	1of M5 is misclassified as a M3

Here TMIs represents total wrongly classified instances and MIs represents misclassified instances in Eq. 1. Therefore, total wrongly predicted test samples are 8. Among 8 samples, one sample is from L2, one sample is L3, two samples are from M2, two samples are from M3 and remaining two samples are from M5 class respectively. After the successful execution of experiment 2, the obtained result of module 2 is shown in Table 5.

From the Table 5, it can be noticed that OCA rises to 94.2% (132/140) for six-classed classifier i.e. 132 of 140 test

Table 5 Performance of secondary classifier: PCA-NN1 to PCA-NN15

	CM						Accuracy (%)						
	L1	L2	L3	M2	M3	M5	OCA	ICA_{L1}	ICA_{L2}	ICA_{L3}	ICA_{M2}	ICA_{M3}	ICA_{M5}
L1	32	0	0	0	0	0	94.2	100	100	93.3	92.5	89.4	91.6
L2	0	22	0	1	0	0							
L3	1	0	14	0	0	0							
M2	0	0	1	25	1	0							
M3	0	0	1	0	17	1							
M5	0	0	0	1	1	22							

Table 6 Misclassified test instances for classification

Experiments	Class name	Total no. of sample	Misclassified instances	TMIs
Experiment 1	L1	30	2	19
	L2	20	3	
	L3	13	2	
	M2	23	4	
	M3	16	3	
	M5	19	5	
Experiment 2	L1	32	0	8
	L2	22	1	
	L3	14	1	
	M2	25	2	
	M3	17	2	
	M5	22	2	

Table 7 Comparative analysis of results

Experiment no	Accuracy (%)	TMI_ Accuracy (%)	PPV (%)	TPR (%)
Experiment 1	86.4	13.6	93.7	96.7
Experiment 2	94.2	5.8	100	96.9

instances are classified accurately. The ICA observed to be 100% (32/32), 100% (22/22), 93.3% (14/15), 92.5% (25/27), 89.4% (17/19) and 91.5% (22/24) for L1, L2, L3, M2, M3 and M5 respectively.

3.2.5.3 Misclassification analysis Table 6 describes the misclassified test instances observed in experiments 1 and 2.

From the Table 6, it can be noticed that 19 test instances are inaccurately classified by module 1.Whereas only 8 test instances are inaccurately classified by module 2. Eight misclassified instances comprise of 1 instance of L2, one instance of L3, two instances of M2, two instances of M3 and two instances of M5. It should be noticed that every test instance of L1 is classified accurately by module 2.

3.2.5.4 Comparative analysis The comparative analysis of extensive experiments carried out for this work is done on the basis of classification accuracy, Positive Predictive Value (PPV), True Positive Rate (TPR) and misclassification accuracy. The mathematical expression for PPV and TPR are is given in Eq. 2 and Eq. 3.

$$PPV = \frac{TP}{TP + FP} \times 100 \tag{2}$$

$$TPR = \frac{TP}{TP + FN} \times 100 \tag{3}$$

where TP: True positive samples, FP: false positive samples, FN: False negative samples.

The comparative analysis of results is given in Table 7.

The graphical representation of obtained results for both experiments shown is shown in Fig. 19.

After the comparative analysis of results obtained from the experiment 1 and experiment 2, shows that the experiment 2 provides better results and suitable for the clinical environment. Therefore, the proposed CAC system for the six-class acute leukemia classification is shown in Fig. 20.

4 Conclusion

The suspicion of acute leukemia can be confirmed by microscopic analysis of bone marrow by hematologist which is a tedious task. In order to automate the process and to assist

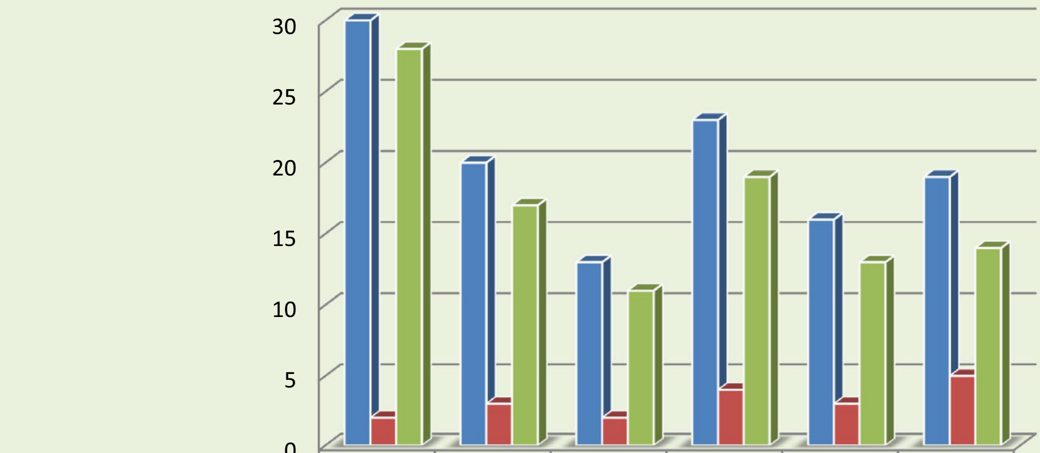

	L1	L2	L3	M2	M3	M5
Total no. of sample	30	20	13	23	16	19
Misclassified instances	2	3	2	4	3	5
Correctly classified Instances	28	17	11	19	13	14

Result analysis of Experiment 1 (PCA-NN0, Acc: 86.4 %)

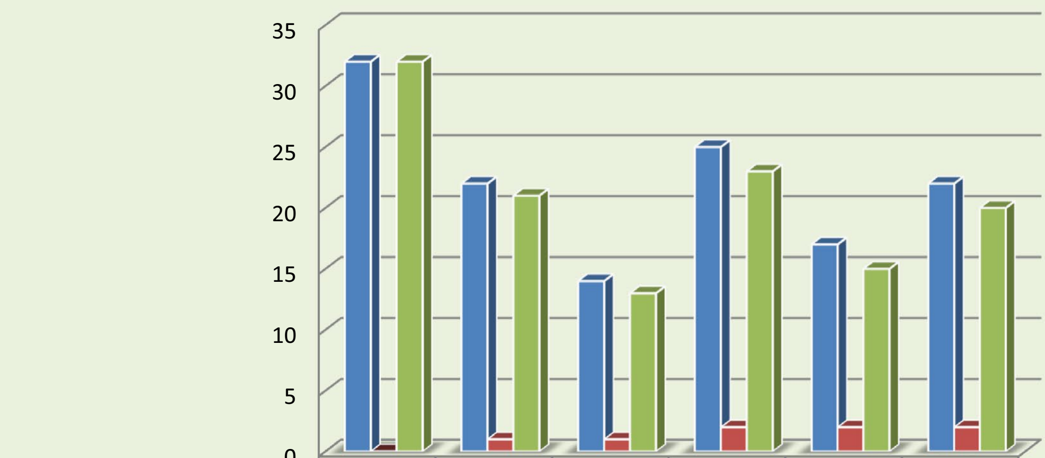

	L1	L2	L3	M2	M3	M5
Total no. of sample	32	22	14	25	17	22
Misclassified instances	0	1	1	2	2	2
Correctly classified Instances	32	21	13	23	15	20

Result analysis of Experiment 2. ((PCA-NN1 to PCA-NN15, Acc: 94.2 %)

Fig. 19 Comparative analysis of results

the expert, there is a requirement of computer-aided classification tool that would be able to distinguish the widespread subset of acute leukemia into its FAB classes. This work gives an automated classifier for acute leukemic cells based on an ensemble of binary ANN classification methods. The accuracy of 86.4% is achieved using single six-class PCA based ANN classifier. These test instances are further classified by the ensemble of binary neural network which yields the 94.2% accuracy. Proposed work administered by hematologist can be utilized for detection of acute leukemia from a set of input data set of images, can distinguish the data of leukemic images from normal images and can further classify these acute leukemic pronounced images into various subtypes.

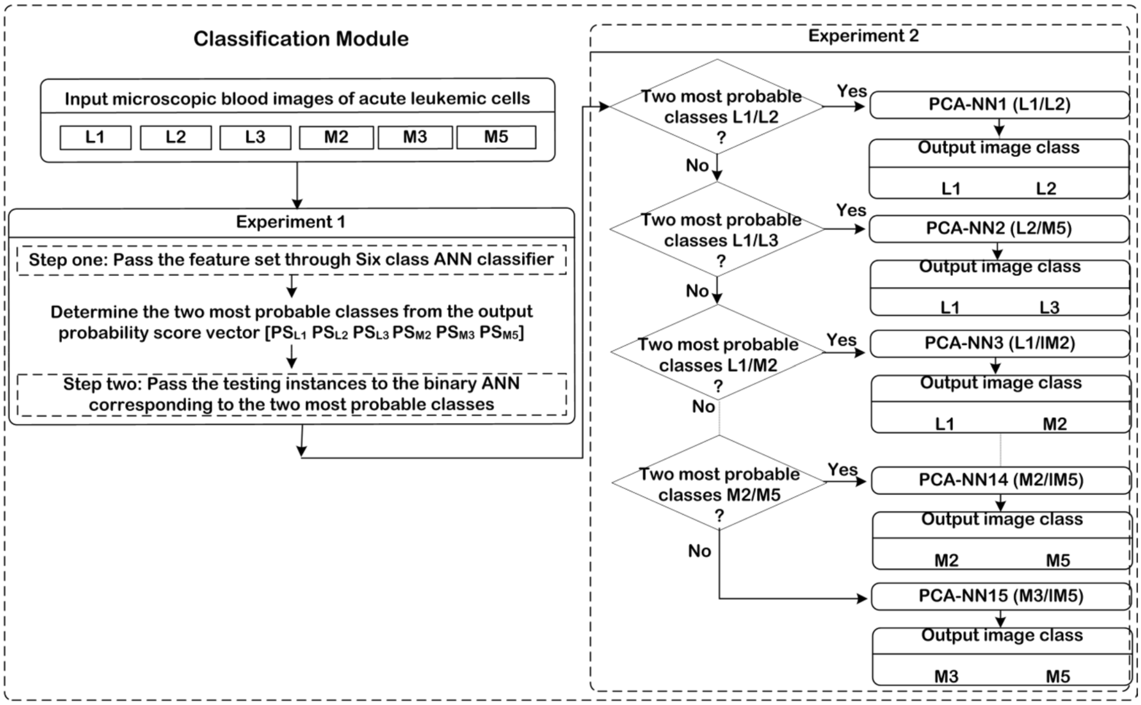

Fig. 20 Proposed classification framework for six-class Acute leukemia classification

References

1. Bain BJ, Bates I, Laffan MA (2016) Dacie and lewis practical haematology e-book. Elsevier Health Sciences
2. Online source: Khan Academy. Inc., a 501(c) (3) organization
3. Rawat J, Singh A, Bhadauria HS, Virmani J, Devgun JS (2017) Classification of acute lymphoblastic leukaemia using hybrid hierarchical classifiers. Multimed Tools Appl 76(18):19057–19085
4. Pedreira CE, Macrini L, Land MG, Costa ES (2009) New decision support tool for treatment intensity choice in childhood acute lymphoblastic leukemia. IEEE Trans Inf Technol B 13(3):284–290
5. Viswanathan P, Fuzzy C (2015) Means detection of leukemia based on morphological contour segmentation. Proc Comput Sci 31(58):84–90
6. Singh G, Bathla G, Kaur S (2016) Design of new architecture to detect leukemia cancer from medical images. Int J Appl Eng Res 11(10):7087–7094
7. Zhang L, Wang QG, Qi JP (2006) Processing technology in microscopic images of cancer cells in pleural fluid based on fuzzy edge detection method. J Phys: Conf Series 48(1):329
8. Amin MM, Kermani S, Talebi A, Oghli MG (2015) Recognition of acute lymphoblastic leukemia cells in microscopic images using K-means clustering and support vector machine classifier. J Med Signals Sens 5(1):49
9. Neoh SC, Srisukkham W, Zhang L, Todryk S, Greystoke B, Lim CP, Hossain MA, Aslam N (2015) An intelligent decision support system for leukaemia diagnosis using microscopic blood images. Sc Rep 5:14938
10. Nasir AA, Mashor MY, Hassan R (2013) Classification of acute leukaemia cells using multilayer perceptron and simplified fuzzy ARTMAP neural networks. Int Arab J Inform Technol 10(4):356–364
11. Bhattacharjee R, Saini LM (2015) Robust technique for the detection of Acute Lymphoblastic Leukemia. In: 2015 IEEE power, communication and information technology conference (PCITC) 15 Oct 2015, pp 657–662. IEEE
12. Mohapatra S, Patra D (2010) Automated cell nucleus segmentation and acute leukemia detection in blood microscopic images. In: Systems in medicine and biology (ICSMB), 2010 international conference on 16 Dec 2010, pp 49–54. IEEE
13. Mohapatra S, Patra D (2010) Automated leukemia detection using hausdorff dimension in blood microscopic images. In: Emerging trends in robotics and communication technologies (INTERACT), 2010 International conference on 3 Dec 2010, pp 64–68. IEEE
14. Mohapatra S, Patra D, Satpathy S (2014) An ensemble classifier system for early diagnosis of acute lymphoblastic leukemia in blood microscopic images. Neural Comput Appl 24(7–8):1887–1904
15. Singhal V, Singh P (2016) Texture features for the detection of acute lymphoblastic leukemia. In: Proceedings of international conference on ict for sustainable development 2016. Springer, Singapore, pp 535–543
16. Mohapatra S, Patra D, Kumar S, Satpathy S (2012) Lymphocyte image segmentation using functional link neural architecture for acute leukemia detection. Biomed Eng Lett 2(2):100–110
17. Madhloom HT, Kareem SA, Ariffin H (2012) A robust feature extraction and selection method for the recognition of Lymphocytes versus acute Lymphoblastic Leukemia. In: Advanced computer science applications and technologies (ACSAT), 2012 international conference on 26 Nov 2012, pp 330–335. IEEE
18. Putzu L, Caocci G, Di Ruberto C (2014) Leucocyte classification for leukaemia detection using image processing techniques. Artif Intell Med 62(3):179–191
19. Putzu L, Di Ruberto C (2013) White blood cells identification and classification from leukemic blood image. In: Proceedings of the IWBBIO international work-conference on bioinformatics and biomedical engineering, 2013 Mar, pp 99–106

20. Rawat J, Singh A, Bhadauria HS, Virmani J (2015) Computer aided diagnostic system for detection of leukemia using microscopic images. Proc Comput Sci 31(70):748–756
21. Scotti F (2005) Automatic morphological analysis for acute leukemia identification in peripheral blood microscope images. In: 2005 IEEE international conference on computational intelligence for measurement systems and applications, 20 Jul 2005, vol 2005, pp 96–101
22. Goutam D, Sailaja S (2015) Classification of acute myelogenous leukemia in blood microscopic images using supervised classifier. In: Engineering and technology (ICETECH), 2015 IEEE international conference on 20 Mar 2015, pp 1–5. IEEE
23. Agaian S, Madhukar M, Chronopoulos AT (2014) Automated screening system for acute myelogenous leukemia detection in blood microscopic images. IEEE Syst J 8(3):995–1004
24. Priya DK, Krithiga SR, Pavithra P, Kumar JR (2015) Detection of leukemia in blood microscopic images using fuzzy logic. Int J Engg Res Sci Tech 240:197–205
25. Kazemi F, Najafabadi TA, Araabi BN (2016) Automatic recognition of acute myelogenous leukemia in blood microscopic images using K-means clustering and support vector machine. J Med Signals Sens 6(3):183
26. Madhloom HT, Kareem SA, Ariffin H (2015) Computer-aided acute leukemia blast cells segmentation in peripheral blood images. J Vibroeng 17(8):4517–4532
27. Belacel N, Vincke P, Scheiff JM, Boulassel MR (2001) Acute leukemia diagnosis aid using multicriteria fuzzy assignment methodology. Comput Methods Prog Bio 64(2):145–151
28. Gonzalez JA, Olmos I, Altamirano L, Morales BA, Reta C, Galindo MC, Alonso JE, Lobato R (2011) Leukemia identification from bone marrow cells images using a machine vision and data mining strategy. Intell Data Anal 15(3):443–462
29. Reta C, Altamirano L, Gonzalez JA, Diaz-Hernandez R, Peregrina H, Olmos I, Alonso JE, Lobato R (2015) Correction: segmentation and classification of bone marrow cells images using contextual information for medical diagnosis of acute leukemias. PLoS ONE 10(7):e0134066
30. Bigorra L, Merino A, Alferez S, Rodellar J (2017) Feature analysis and automatic identification of leukemic lineage blast cells and reactive lymphoid cells from peripheral blood cell images. J Clin Lab Anal 31(2):e22024
31. ASH Image Bank: American Society of Hematology. https://imagebank.hematology.org
32. Labati RD, Piuri V and Scotti F (2011) All-IDB: the acute lymphoblastic leukemia image database for image processing. In: Image processing (ICIP), 2011 18th IEEE international conference on, pp 2045–2048. IEEE
33. Rawat J, Singh A and Bhadauria HS (2014). An approach for leukocytes nuclei segmentation based on image fusion. In: Signal processing and information technology (ISSPIT), 2014 IEEE international symposium on, pp 000456–000461. IEEE
34. Haralick RM, Shanmugam K (1973) Textural features for image classification. IEEE Trans Syst Man Cybern 6:610–621
35. Laws KI (1980). Rapid texture identification. In: 24th annual technical symposium, pp 376–381. International Society for Optics and Photonics
36. Lee CC and Chen SH (2006). Gabor wavelets and SVM classifier for liver diseases classification from CT images. In: 2006 IEEE international conference on systems, man and cybernetics, vol 1, pp 548–552. IEEE
37. Mingqiang Y, Kidiyo K, Joseph R (2008) A survey of shape feature extraction techniques. Pattern Recogn 15(7):43–90
38. Bengtsson T (2008) Classification of cell images using MPEG-7-influenced descriptors and support vector machines in cell morphology. Institutionen för datavetenskap, Lundsuniversitet
39. Chris A, Mulyawan B (2012) A combination of feature selection and co-occurrence matrix methods for leukocyte recognition system. J Softw Eng Appl 5:101
40. Rawat J, Bhadauria HS, Singh A and Virmani J (2015). Review of leukocyte classification techniques for microscopic blood images. In: Computing for sustainable global development (INDIACom), 2015 2nd International Conference on, pp 1948–1954. IEEE
41. Kriti, Virmani J (2015) Breast density classification using Laws' mask texture features. Int J Biomed Eng Technol 19(3):279–302
42. Han ZY, Gu DH, Wu QE (2016) Feature extraction for color images. Electronics communications and networks. Springer, Singapore, pp 215–221
43. Khan S, Hussain M, Aboalsamh H, Bebis G (2017) A comparison of different Gabor feature extraction approaches for mass classification in mammography. Multimed Tools Appl 76(1):33–57
44. Rawat J, Singh A, Bhadauria HS, Virmani J, Devgun JS (2018) Application of ensemble artificial neural network for the classification of white blood cells using microscopic blood images. Int J Comput Syst Eng 4(2–3):202–216
45. Cornfield JEROME (1972) Statistical classification methods. In: Proceedings of the second conference on the diagnostic process, computer diagnosis and diagnostic methods, Chicago, pp 108–130
46. Devijver PA, Kittler J (1982) Pattern recognition: a statistical approach. Prentice hall, New Jersey
47. Fukunaga K (2013) Introduction to statistical pattern recognition. Elsevier, Amsterdam
48. Jiang J, Trundle P, Ren J (2010) Medical image analysis with artificial neural networks. Comput Med Imaging Graph 34(8):617–631
49. Virmani J, Kumar V, Kalra N, Khandelwal N (2014) Neural network ensemble based CAD system for focal liver lesions from B-mode ultrasound. J Digit Imaging 27(4):520–537
50. Singh PP and Garg RD (2011) Land use and land cover classification using satellite imagery: a hybrid classifier and neural network approach. In: Proceedings of international conference on advances in modeling, optimization and computing (AMOC-2011), pp 753–762
51. Rawat J, Singh A, Bhadauria HS, Virmani J, Devgun JS (2017) Computer assisted classification framework for prediction of acute lymphoblastic and acute myeloblastic leukemia. Biocybern Biomed Eng 37(4):637–654
52. Rawat J, Singh A, Bhadauria HS and Kumar I (2014). Comparative analysis of segmentation algorithms for leukocyte extraction in the acute Lymphoblastic Leukemia images. In: Parallel, distributed and grid computing (PDGC), 2014 international conference on, pp 245–250. IEEE
53. Kurita T, Otsu N, Abdelmalek N (1992) Maximum likelihood thresholding based on population mixture models. Pattern Recogn 25(10):1231–1240
54. Kwon SH (2004) Threshold selection based on cluster analysis. Pattern Recogn Lett 25(9):1045–1050
55. Bieniek A, Moga A (2000) An efficient watershed algorithm based on connected components. Pattern Recogn 33(6):907–916
56. Saarinen K (1994). Color image segmentation by a watershed algorithm and region adjacency graph processing. In: Image processing, 1994. Proceedings. ICIP-94., IEEE international conference, vol 3, pp 1021–1025
57. Rawat J, Singh A, Bhadauria HS, Virmani J (2015) Computer aided diagnostic system for detection of leukemia using microscopic images. Proc Comput Sci 70:748–756
58. Rawat J, Singh A, Bhadauria HS, Virmani J, Devgun JS (2017) Leukocyte classification using adaptive neuro-fuzzy inference system in microscopic blood images. Arab J Sci Eng 8:1–18
59. Ladines-Castro W, Barragan-Ibanez G, Luna-Perez MA, Santoyo-Sanchez A, Collazo-Jaloma J, Mendoza-García E,

Ramos-Penafiel CO (2016) Morphology of leukaemias. Rev Med Hosp Gener de Mex 79(2):107–113
60. El Houby EM (2018) Framework of computer aided diagnosis systems for cancer classification based on medical images. J Med Syst 42(8):157
61. Alsalem MA, Zaidan AA, Zaidan BB, Albahri OS, Alamoodi AH, Albahri AS, Mohsin AH, Mohammed KI (2019) Multiclass benchmarking framework for automated acute Leukaemia detection and classification based on BWM and group-VIKOR. J Med Syst 43(7):212
62. Kurniadi FI, Putri VK (2019) A comparison of human crafted features and machine crafted features on white blood cells classification. J Phys: Conf Series 1201(1):012045
63. Salman OH, Zaidan AA, Zaidan BB, Naserkalid, Hashim M (2017) Novel methodology for triage and prioritizing using "big data" patients with chronic heart diseases through telemedicine environmental. Int J Inform Technol Decis Making 16(05):1211–1245
64. Kalid N, Zaidan AA, Zaidan BB, Salman OH, Hashim M, Albahri OS, Albahri AS (2018) Based on real time remote health monitoring systems: A new approach for prioritization "large scales data" patients with chronic heart diseases using body sensors and communication technology. J Med Syst 42(4):69
65. Mohsin AH, Zaidan AA, Zaidan BB, Albahri OS, Albahri AS, Alsalem MA, Mohammed KI (2019) Based medical systems for patient's authentication: Towards a new verification secure framework using CIA standard. J Med Syst 43(7):192
66. Mohsin AH, Zaidan AA, Zaidan BB, bin Ariffin SA, Albahri OS, Albahri AS, Alsalem MA, Mohammed KI, Hashim M (2018) Real-time medical systems based on human biometric steganography: a systematic review. J Med Syst 42(12):245
67. Albahri OS, Albahri AS, Mohammed KI, Zaidan AA, Zaidan BB, Hashim M, Salman OH (2018) Systematic review of real-time remote health monitoring system in triage and priority-based sensor technology: taxonomy, open challenges, motivation and recommendations. J Med Syst 42(5):80
68. Liang G, Hong H, Xie W, Zheng L (2018) Combining convolutional neural network with recursive neural network for blood cell image classification. IEEE Access 6:36188–36197
69. Macawile MJ, Quiñones VV, Ballado A, Cruz JD and Caya MV(2018). White blood cell classification and counting using convolutional neural network. In: 2018 3rd International conference on control and robotics engineering (ICCRE), pp 259–263. IEEE
70. Hegde RB, Prasad K, Hebbar H, Singh BMK (2019) Comparison of traditional image processing and deep learning approaches for classification of white blood cells in peripheral blood smear images. Biocybern Biomed Eng 39(2):382–392
71. Choi JW, Ku Y, Yoo BW, Kim JA, Lee DS, Chai YJ, Kong HJ, Kim HC (2017) White blood cell differential count of maturation stages in bone marrow smear using dual-stage convolutional neural networks. PLoS ONE 12(12):e0189259
72. Vogado LH, Veras RM, Araujo FH, Silva RR, Aires KR (2018) Leukemia diagnosis in blood slides using transfer learning in CNNs and SVM for classification. Eng Appl Artif Intell 72:415–422
73. Rehman A, Abbas N, Saba T, Rahman SIU, Mehmood Z, Kolivand H (2018) Classification of acute lymphoblastic leukemia using deep learning. Microsc Res Tech 81(11):1310–1317
74. Shafique S, Tehsin S (2018) Acute lymphoblastic leukemia detection and classification of its subtypes using pretrained deep convolutional neural networks. Technol Cancer Res Treat 17:1533033818802789
75. Tuba E, Strumberger I, Bacanin N, Zivkovic D and Tuba M (2019). Acute lymphoblastic leukemia cell detection in microscopic digital images based on shape and texture features. In: International conference on swarm intelligence. Springer, Cham, pp 142–151
76. Acevedo A, Alférez S, Merino A, Puigví L, Rodellar J (2019) Recognition of peripheral blood cell images using convolutional neural networks. Comput Methods Progr Biomed 180:105020
77. Jha KK, Dutta HS (2019) Mutual information based hybrid model and deep learning for acute lymphocytic leukemia detection in single cell blood smear images. Comput Methods Progr Biomed 179:104987
78. Kumar I, Bhadauria HS, Virmani J, Thakur S (2017) A classification framework for prediction of breast density using an ensemble of neural network classifiers. Biocybern Biomed Eng 37(1):217–228
79. Kumar I, Bhadauria HS, Virmani J (2018) A computerised framework for prediction of fatty and dense breast tissue using principal component analysis and multi-resolution texture descriptors. Int J Comput Syst Eng 4(2–3):73–85